The Meteoritical Society

Meteoritics & Planetary Science 42, Nr 7/8, 1291–1308 (2007)
Abstract available online at http://meteoritics.org

Late accretion and lithification of chondritic parent bodies: Mg isotope studies on fragments from primitive chondrites and chondritic breccias

Anna K. SOKOL[1, 3*], Addi BISCHOFF[1], Kuljeet K. MARHAS[2], Klaus MEZGER[3], and Ernst ZINNER[2]

[1]Institut für Planetologie, Wilhelm-Klemm-Str. 10, 48149 Münster, Germany
[2]McDonnell Center for the Space Sciences and Physics Department, Washington University, One Brookings Drive, Saint Louis, Missouri 63130, USA
[3]Institut für Mineralogie, Corrensstr. 24, 48149 Münster, Germany
[*]Corresponding author. E-mail: sokola@uni-muenster.de

(Received 16 October 2006; revision accepted 25 July 2007)

Abstract–Recent results of isotopic dating studies (^{182}Hf-^{182}W, ^{26}Al-^{26}Mg) and the increasing number of observed igneous and metamorphosed fragments in (primitive) chondrites provide strong evidence that accretion of differentiated planetesimals predates that of primitive chondrite parent bodies. The primitive chondrites Adrar 003 and Acfer 094 contain some unusual fragments that seem to have undergone recrystallization. Magnesium isotope analyses reveal no detectable radiogenic ^{26}Mg in any of the studied fragments. The possibility that evidence for ^{26}Al was destroyed by parent body metamorphism after formation is not likely because several other constituents of these chondrites do not show any metamorphic features. Since final accretion of a planetesimal must have occurred after formation of its youngest components, formation of these parent bodies must thus have been relatively late (i.e., after most ^{26}Al had decayed). Al-Mg isotope data for some igneous-textured clasts (granitoids and andesitic fragments) within the two chondrite regolith breccias Adzhi-Bogdo and Study Butte reveal also no evidence for radiogenic ^{26}Mg. As calculated from the upper limits, the formation of these igneous clasts, the incorporation into the parent body regolith, and the lithification must have occurred at least 3.8 Myr (andesite in Study Butte) and 4.7 Myr (granitoids in Adzhi-Bogdo) after calcium-aluminum-rich inclusions (CAI) formation. The absence of ^{26}Mg excess in the igneous inclusions does not exclude ^{26}Al from being a heat source for planetary melting. In large, early formed planetesimals, cooling below the closure temperature of the Al-Mg system may be too late for any evidence for live ^{26}Al (in the form of ^{26}Mg excess) to be preserved. Thus, growing evidence exists that chondritic meteorites represent the products of a complex, multi-stage history of accretion, parent body modification, disruption and re-accretion.

INTRODUCTION

Chondrites are traditionally considered to represent the most primitive and oldest objects in the solar system. However, it has also been suggested that certain chondritic meteorites could represent samples of "second-generation" parent bodies (daughter asteroids) resulting from collisional destruction of "grandparent planetary bodies" (e.g., Urey 1959 and 1967; Zook 1980; Hutchison et al. 1988; Hutcheon and Hutchison 1989; Hutchison 1996; Sanders 1996; Bischoff 1998; Bischoff and Schultz 2004; Kleine et al. 2005a, 2005b; Bischoff et al. 2006).

Recent studies show increasing evidence for the existence of planetesimals before the accretion of the parent asteroids of chondrites. Based on a comparison of the abundances of ^{182}W, the decay product of the short-lived isotope ^{182}Hf (half-life = 9 Myr), in several iron meteorites and in calcium-aluminum-rich inclusions (CAIs), Kleine et al. (2004, 2005a, 2005b) and Markowski et al. (2006) concluded that most magmatic iron meteorites formed within less than ~1 Myr after the formation of CAIs. Combining age constraints derived from the Hf-W and Al-Mg systems Kleine et al. (2004, 2005a, 2005b) argued that certain iron meteorites may have originated from the earliest accreted asteroids. This in turn implies that most chondrites have to derive from relatively late-formed bodies. Srinivasan et al. (1999), Baker et al. (2005), and Bizzarro et al. (2005) reported ^{26}Mg excesses resulting from the decay of ^{26}Al in bulk samples

from some achondritic meteorites (angrites, eucrites, mesosiderites). Based on these results, they argued that parent bodies of these meteorites melted while ^{26}Al and ^{60}Fe were still abundant enough to drive asteroid melting. Thermal modeling based on these heat sources shows that accretion of these differentiated bodies must have been completed within <1.5 Myr after the CAIs had formed (Haack et al. 2005; Sanders and Taylor 2005). Since most chondrules postdate CAI formation by about 2 Myr (e.g., Russell et al. 1996; Kita et al. 2000, 2005; Huss et al. 2001; Amelin et al. 2002; Kunihiro et al. 2004; Mostefaoui et al. 2002), accretion of some achondritic parent bodies must have predated accretion of chondrite parent bodies. Furthermore, Baker and Bizzarro (2005) reported ^{26}Mg deficits in differentiated meteoritic material with Al/Mg ~ 0 (aubrites, ureilites, and pallasites). Model ages calculated from these deficits are older than those of most chondrules from chondritic meteorites. Again, these results support the conclusion that accretion of differentiated meteorites predates that of chondrule-bearing meteorites. A consequence of all these studies is that chondritic planetesimals accreted when ^{26}Al was no longer available in sufficient amounts to drive melting. These planetesimals may have formed by re-accretion of debris produced during collisional disruption of old first-generation planetesimals.

If this is true, fragments of these earlier bodies may be mixed with later-formed chondrules and should exist in primitive chondrites or breccias. Indeed, the increasing number of planetary igneous fragments observed within (primitive) chondrites strongly suggests that differentiated meteorites come from bodies that accreted and differentiated before the chondrite parent bodies.

Igneous-textured fragments have been reported from several chondrites (e.g., Julesberg [L3], Vishnupur [LL4–6]; Ruzicka et al. 1998; Bridges and Hutchison 1997). It has also been suggested that a microgabbro in the Parnallee chondrite formed by partial melting in a planetary body after the removal of metallic Fe (Kennedy et al. 1992). Bridges et al. (1995b) described a feldspar-nepheline achondritic clast in Parnallee that has an O-isotopic composition indicating carbonaceous chondrite affinities. Several other large achondritic clasts include pyroxenitic or noritic fragments in Hedjaz (L3.7) (Nakamura et al. 1990; Misawa et al. 1992), troctolitic and/or dunitic and/or harzburgitic inclusions in Barwell (L6), Yamato (Y-) 75097 (L6), Y-794046 (H5), and Y-793241 (e.g., Prinz et al. 1984; Hutchison et al. 1988; Nagao 1994; Mittlefehldt et al. 1995).

Igneous-textured fragments with abundant SiO_2 phases (quartz, cristobalite, tridymite) occur in several ordinary chondrites (e.g., Wlotzka et al. 1983; Bischoff 1993; Bischoff et al. 1993, 2006; Bridges et al. 1995a; Ruzicka et al. 1995; Hezel 2003). Significant differentiation of chondritic material is required to form the silica-oversaturated liquids from which such rocks could have crystallized. The result can, for example, be coarse-grained granitoidal clasts such as those found in the Adzhi-Bogdo LL3–6 chondrite (Bischoff 1993; Bischoff et al. 1993). Clasts consisting of up to 95 vol% of a SiO_2 phase were described from the meteorites Parnallee (LL3) and Farmington (L5) (Bridges et al. 1995a). In addition, a clast with SiO_2-normative mesostasis was found in the Hammadah al Hamra 180 unique chondrite with affinity to LL group ordinary chondrites (Bischoff et al. 1997). The presence of excess ^{26}Mg in some of these igneous fragments (e.g. CC-1 from Semarkona) indicates that planetary bodies accreted early and incorporated a substantial amount of ^{26}Al (Hutcheon and Hutchison 1989). Thus, decay of ^{26}Al most likely provided the heat energy required for melting and high grade metamorphism.

In this study, possibly old lithic components occurring as foreign clasts within primitive chondrites (Adrar 003, Acfer 094) and chondrite regolith breccias (Adzhi-Bogdo, Study Butte) (Sokol and Bischoff 2006) were analyzed. Based on their textures, these fragments may represent clasts of precursor planetesimals. They must have formed through igneous processes or were modified through thermal metamorphism. The thermal overprint (melting and metamorphism) of all these fragments must have occurred at a much higher temperature than that experienced by their current matrix. These fragments were thus part of bodies with a high-temperature evolution prior to their incorporation into the present chondrites.

The main goal of this study is to obtain relative ages on these fragments using the Al-Mg isotope systematics. Since all evidence of "older" differentiated objects comes from model ages, the present study was focused on direct evidence of early forming parent bodies from isochron ages. The short-lived radionuclide ^{26}Al (half-life = 0.73 Myr) is useful as a chronometer in establishing time differences between important events in the solar nebula and early formed solids differing by only a few million years. The former presence of ^{26}Al can now be observed as an excess of ^{26}Mg, its decay product. Given a homogeneous distribution of ^{26}Al in the solar nebula, differences in inferred initial $^{26}Al/^{27}Al$ ratios can give information about relative formation times.

ANALYTICAL PROCEDURES

Polished thin sections of all meteorites were studied by optical microscopy in transmitted and reflected light. A JEOL 840A scanning electron microscope (SEM) was used to resolve the fine-grained texture of the rocks as well as to locate grains of feldspar with sizes suitable for ion probe analysis. Mineral analyses were obtained with a JEOL JXA-8600 S electron microprobe operating at 15 kV and a probe current of 15 nA. All data were corrected using the atomic number (Z), absorption (A), and fluorescence (F) (ZAF) correction procedures.

Magnesium isotope ratios and Al/Mg ratios were measured by secondary ion mass spectrometry (SIMS) using the Cameca IMS 3f instrument and the NanoSIMS ion microprobe at Washington University in Saint Louis,

Missouri, USA. Feldspar grains in granitoidal fragments from Adzhi-Bogdo are large enough (>20 μm) for analysis with the Cameca IMS 3f. Two of these fragments were measured with this instrument. The primary ion beam of $^{16}O^-$ impinged on the sample surface with an energy of 17 keV. The current of the focused beam was ~3.0 nA and resulted in a primary beam spot with a diameter of about 10–15 μm. The Mg ions were collected by an electron multiplier (EM) in peak jumping mode. The ^{27}Al ions were collected with a Faraday cup sequentially with the Mg isotopes. A mass resolving power of ≈3500 was sufficient to eliminate all significant interferences ($^{48}Ca^{++}$, MgH).

The small sizes of feldspar grains and/or the existence of fractures in grains from all other inclusions (from Acfer 094, Adrar 003, and Study Butte) resulted in useful areas that are only a few micrometers in diameter. As a consequence of this small grain size, the NanoSIMS ion microprobe had to be used for these analyses. This instrument, with its high lateral resolution and its high transmission, is well-suited for the analysis of feldspar grains (Zinner et al. 2002). However, the presence of many tiny Mg-rich grains in the plagioclase and the surrounding Mg-rich phases complicated the analyses (compare Table 1). In order to avoid the high Mg signal originating from inclusions and surrounding phases, "clean" areas were selected, and Al and Mg ion images were observed before each analysis. In spite of these precautions, the primary beam frequently sputtered in Mg-rich phases, shortening the useful analysis time. The relatively large analytical uncertainties are the result of the unusual heterogeneity of the samples and the short measurement times and are not inherent in the analytical method. Short measurement times resulting in small total counts and heterogeneity resulting in variations in the count rates between measurement cycles contributed to the uncertainties. Both errors based on Poisson counting statistics as well as errors based on variations of isotopic ratios between measurement cycles were evaluated. The larger error was chosen.

An $^{16}O^-$ primary ion beam with a current of ~30–50 pA and an energy of 16 keV was used to generate positive secondary ions for the analyses. The typical beam diameter was 2–4 μm. The measurements were carried out with a mass resolving power of ~4000. Magnesium isotopes were measured in a peak jumping mode, while Al^+ was detected simultaneously (multi-detection mode). Due to very high count rates of $^{27}Al^+$ in some cases, $^{27}Al/^{24}Mg$ ratios were determined independently before and after the measurement of the Mg isotope ratio.

Although the NanoSIMS offers the possibility of multidetection of the Mg isotopes, the peak jumping mode was chosen. The reason is that the detection efficiency varies among the different electron multiplier detectors and thus calibration measurements on a calibration phase are necessary. Such calibrations are generally performed on other meteoritic phases such as pyroxene or olivine, which have high Mg concentrations. In addition, such measurements on phases with low Al/Mg ratios would serve as anchor points for the Al-Mg isochrons. However, this was not possible because of the quasi-simultaneous arrival (QSA) effect (Slodzian et al. 2004), which affected the analyses. The probability that a single primary ion produces more than one secondary ion is not negligible. In the NanoSIMS, which has a very high collection and transmission of secondary ions, it is possible that two ions with the same mass arrive with such a small time difference at the electron multiplier detector that they can be detected only as a single pulse. Since in the case of Mg the number of incidences where the two ions are both from ^{24}Mg is much higher than for the other isotopes, ^{24}Mg is systematically undercounted. As a result, $^{25}Mg/^{24}Mg$ and $^{26}Mg/^{24}Mg$ are too high by the same factor and, after fractionation correction based on the $^{25}Mg/^{24}Mg$ ratio, results in a negative $\delta^{26}Mg$ value. The QSA effect is only observed in samples with high concentrations of an element with high ionization efficiency. In sulfides, the QSA effect for S can be as large as 20% (Slodzian et al. 2004). Indeed, in contrast to measurements on pyroxene using the IMS 3f, NanoSIMS measurements on pyroxene ($^{27}Al/^{24}Mg < 0.01$) made by peak jumping yielded negative $\delta^{26}Mg$ values with an average of $\delta^{26}Mg = -6.8 \pm 3.0$ (2σ). However, in the plagioclase analyzed in this work, in which the Mg concentrations are lower than in the pyroxene by at least a factor of 40, the QSA effect is completely negligible. NanoSIMS analyses on two terrestrial plagioclase standards, with $^{27}Al/^{24}Mg$ ratios of 390 and 640, yielded an average of $\delta^{26}Mg = -1.5 \pm 2.7$ (2σ), which is isotopically normal within the experimental uncertainties. As a consequence, no NanoSIMS measurements on high-Mg phases were used and the Al-Mg isochrons were obtained by forcing the line through the terrestrial $^{26}Mg/^{24}Mg$ ratio at Al/Mg = 0.

For both instruments, the reference value used for $^{25}Mg/^{26}Mg$ was 0.12663 and 0.13932 for $^{26}Mg/^{24}Mg$ (Catanzaro et al. 1966). The nonlinear excess in ^{26}Mg ($\delta^{26}Mg$) was calculated assuming a linear mass fractionation law:

$$\delta^{26}Mg = \Delta^{26}Mg - (2 \times \Delta^{25}Mg) \quad (1)$$

where $\Delta^i Mg = ([^iMg/^{24}Mg]_{measured}/[^iMg/^{24}Mg]_{reference} - 1) \times 1000$ (per mil); (i = 25, 26).

The measured $^{27}Al/^{24}Mg$ ratios were corrected for the relative sensitivity factor determined from a terrestrial plagioclase standard (Miyakejima plagioclase).

RESULTS

Characterization of the Meteorites Acfer 094, Adzhi-Bogdo, Study Butte, and Adrar 003 and Selected Fragments

Acfer 094

This is a unique, type 3 carbonaceous chondrite that was first classified as a CO(CM) chondrite (Bischoff et al. 1991; Wlotzka 1991). Bischoff and Geiger (1994) suggested that it

Table 1. Electron microprobe analyses of feldspars.

	SiO_2	TiO_2	Al_2O_3	FeO	MnO	MgO	CaO	Na_2O	K_2O	Cr_2O_3	Total	An
AB #4[a]	64.6	0.05	18.5	0.16	–	<0.4	<0.02	0.43	16.3	–	100.0	0
AB #5	67.1	–	17.1	0.25	0.02	0.03	<0.03	0.60	15.0	–	100.1	0
A094 #1	45.0	<0.01	35.1	0.52	0.01	0.57	19.9	0.05	–	–	101.2	99.6
	45.5	<0.03	34.2	0.31	0.04	0.71	19.8	0.06	<0.01	<0.06	100.6	99.4
	47.2	<0.01	33.4	0.37	0.07	0.81	19.2	0.11	<0.02	<0.02	101.2	98.9
	44.3	–	34.8	0.95	–	0.59	19.7	0.06	–	<0.02	100.4	99.5
	46.6	<0.01	32.5	0.41	0.01	0.88	19.2	0.10	<0.02	–	99.7	98.9
A094 #2	45.0	<0.02	32.7	2.2	–	0.79	17.8	0.85	<0.04	<0.02	99.3	91.8
	46.6	<0.04	33.8	1.1	–	0.80	18.6	0.35	<0.01	–	101.3	96.7
	46.2	0.07	33.8	0.40	–	0.77	19.0	0.49	<0.01	<0.07	100.7	95.5
	46.5	<0.03	34.0	0.46	–	0.84	19.1	0.45	–	–	101.4	95.9
A094 #3	47.1	–	31.8	0.32	0.01	0.99	18.6	0.70	<0.01	–	99.5	93.5
	47.6	<0.01	32.1	0.34	0.07	0.80	18.1	0.74	0.05	–	99.8	92.9
	48.6	–	31.8	0.54	0.05	0.90	17.4	1.4	<0.01	<0.05	100.7	87.2
	47.8	<0.02	31.4	0.42	0.08	0.94	17.9	1.1	<0.01	<0.06	99.6	89.9
A094 #10	44.9	–	36.5	0.40	–	0.09	19.6	0.07	<0.01	–	101.6	99.3
	44.2	<0.01	36.3	0.40	–	0.37	19.4	0.06	–	<0.02	100.7	99.5
A094 #4	44.8	–	34.7	0.10	0.02	0.49	19.8	0.05	<0.01	<0.04	100.0[b]	99.5
	44.3	<0.03	35.4	0.11	–	0.4	19.8	0.10	–	–	100.0[b]	99.1
	45.6	–	34.1	0.31	–	0.59	19.3	0.08	–	0.10	100.0[b]	99.2
	45.6	<0.02	34.1	0.21	–	0.59	19.5	0.09	–	<0.02	100.0[b]	99.2
A094 #5	47.1	–	34.5	0.44	–	0.71	18.9	0.11	–	–	101.8	98.9
	48.0	0.09	33.3	0.32	0.00	0.79	18.5	0.08	<0.02	0.09	101.2	99.2
	47.8	<0.01	33.8	0.32	0.03	0.87	18.8	0.10	<0.01	–	101.7	99.0
A003 #1	46.0	<0.04	33.9	1.1	0.03	0.36	17.6	0.74	<0.02	<0.05	99.7	92.8
	47.2	<0.01	33.7	1.3	0.04	0.28	17.2	1.0	<0.04	<0.06	100.7	90.0
	49.0	<0.04	33.2	0.98	0.02	0.67	17.3	1.3	<0.01	<0.02	102.5	87.6
A003 #2	46.0	0.09	33.91	0.81	–	0.34	18.0	0.89	<0.01	<0.02	100.0	91.8
	48.5	0.08	33.8	0.64	–	0.54	17.6	1.2	<0.02	–	102.4	88.7
	48.7	<0.02	33.2	0.57	–	0.58	17.6	1.3	–	0.06	102.0	87.7
	48.5	<0.01	33.2	0.61	0.02	0.62	17.5	1.4	<0.01	–	101.9	87.3
	48.2	<0.03	33.1	0.60	–	0.55	17.8	1.2	<0.01	<0.06	101.5	89.4
	47.1	0.06	34.1	1.04	–	0.27	18.1	0.92	–	<0.06	101.6	91.6
A003 #3	46.4	<0.04	33.2	0.99	–	0.46	18.2	1.1	<0.02	<0.02	100.4	90.4
	49.2	0.06	32.1	1.03	–	0.52	17.2	1.8	<0.03	–	101.9	84.1
	48.3	0.06	33.3	1.29	–	0.35	17.7	1.4	<0.02	–	102.4	87.7
A003 #4	46.5	0.01	33.3	2.11	0.01	0.79	17.4	1.1	<0.03	<0.01	101.2	89.3
	48.0	–	33.2	1.49	0.02	0.42	17.6	1.4	–	–	102.1	87.3
	47.1	<0.02	34.2	1.26	–	0.31	18.4	1.1	–	<0.06	102.4	90.7
	47.0	0.06	34.5	0.56	–	0.43	18.7	0.87	–	<0.05	102.1	92.2
SB 1b	57.6	0.06	27.0	–	–	<0.01	9.4	6.0	<0.07	–	100.1	46.0
	56.7	<0.04	27.1	0.84	–	0.05	9.5	5.8	<0.09	–	100.0	47.2
	57.8	0.09	27.3	0.15	–	0.02	9.6	6.2	<0.08	–	101.2	45.8
	63.2	0.23	24.2	0.30	–	0.28	6.0	7.5	0.13	<0.01	101.8	30.5
SB 4a	68.4	0.05	19.7	0.66	<0.01	0.05	1.0	7.5	4.5	0.21	102.1	5.2
	65.0	0.06	21.0	0.41	–	0.02	3.0	8.6	1.1	0.38	99.6	15.2
SB 4e	66.6	<0.01	20.1	0.51	<0.04	<0.01	2.3	9.9	0.57	<0.03	100.1	10.8
	66.6	–	19.9	0.38	0.07	<0.01	2.6	9.9	0.61	<0.01	100.1	12.3
	66.2	–	20.1	0.26	–	–	2.2	9.9	1.0	0.09	99.8	10.2
	67.2	–	19.8	0.27	<0.04	<0.01	2.1	9.9	0.98	<0.10	100.3	10.0

[a]AB =Adzhi Bogdo, A094 = Acfer 094, A003 = Adrar 003, SB = Study Butte; An = anorthite; n.d. = not detected; < = below detection limit.
[b]Normalized to 100%.
All data in wt%. Some feldspar analyses appear to be contaminated by surrounding phases due to their small grain size. This results, for example, in high FeO and MgO contents and slight deviations from stoichiometry.

may be the first CM3 chondrite. However, chemical, mineralogical, and O isotope characteristics are not distinctive enough to distinguish unambiguously between a CO3 and CM2 classification. In addition, the light elements C and N have isotope systematics that do not match those of any other recognized meteorite group (Newton et al. 1995). A transmission electron microscopy (TEM) study revealed that the fine-grained matrix of Acfer 094 consists of an unequilibrated assemblage of amorphous material, tiny forsteritic olivines, low-Ca pyroxenes, and Fe,Ni sulfides (Greshake 1997). Although some similarities to the unequilibrated CO3 chondrite ALHA77307 and the unique type 3 chondrite Kakangari were found, Greshake (1997) stated that Acfer 094 remains unique. The Acfer 094 rock was also characterized as an accretionary breccia (Bischoff et al. 2006). Recently, Grossman and Brearley (2005) suggested that Acfer 094 belongs to the highly primitive carbonaceous chondrites of type 3.0. Thus, this meteorite appears to be a mineralogically pristine rock that escaped thermal metamorphism and aqueous alteration. Its primitive nature is also indicated by very high abundances of presolar SiC and diamonds (Gao et al. 1996) as well as silicates (Nguyen and Zinner 2004; Nguyen et al. 2007).

In addition to the matrix, Acfer 094 consists of abundant chondrules, chondrule fragments, CAIs, amoeboid olivine aggregates, and mineral fragments. Most chondrules contain Fa-poor olivine ($Fa_{<2}$), but olivines in the matrix have a broad peak at $Fa_{37–50}$. Calcium pyroxenes are less abundant than Ca-poor pyroxenes and are compositionally variable ($Fs_{0.4–7.9}Wo_{35.5–46.0}$). Most Ca-poor pyroxenes in the chondrules are enstatites, with Fs content usually below 2 mol%. Pyroxene in the matrix has variable Fs content ($Fs_{1–16}$) (Newton et al. 1995).

This meteorite contains numerous fragments showing metamorphic textures (Figs. 1a and 1b). Although similar objects were described as chondrules (Zanda 2004; Kita personal communication), these irregularly shaped inclusions more likely represent fragments of once-larger thermally recrystallized lithologies. They exhibit a clearly granulitic texture, typically with 120° grain boundary junctions. A granulitic texture requires prolonged annealing, which is not expected to occur in the solar nebula during chondrule formation, but could have taken place on the parent bodies of metamorphosed meteorites (Libourel and Krot 2007).

Mineral constituents of the fragments include pyroxene, olivine, feldspar, and sulfide. Feldspar does not occur interstitially (as in most chondrules), but forms separate large crystals (up to 50 μm in apparent size). Most feldspars are anorthites ($An_{>90}$) (Table 1), but some are more sodic (~An_{70}) (Table 1). Olivine is Fa-poor ($Fa_{1–5}$) and pyroxene is Fs-poor ($Fs_{1–4}$).

Bischoff et al. (2006) described an object in Acfer 094 that is clearly a metamorphosed lithic clast, and which contains a Ca-Al-rich inclusion. The dominant phase in the lithic fragment is Fe-rich olivine (~$Fa_{30–35}$) having 120° grain boundary junctions. Some of the large olivines are still zoned having forsteritic cores (up to ~Fo_{96}). The temperature of the metamorphic episode was not high enough or the duration not long enough for complete equilibration. Similar features are frequently found in CK4 or other type 4 chondrites.

In addition to five metamorphic fragments, one Ca-Al-rich inclusion from Acfer 094 was analyzed in this study. This CAI is a fine-grained intergrowth of forsterite (Fo_{99}), anorthite ($An_{98–100}$), Al-Ti–bearing Ca-pyroxene, and traces of Fe,Ni metal (Fig. 1f). Within the Ca-pyroxene, Al_2O_3 and TiO_2 concentrations of 6–12 wt% and 1–4 wt%, respectively, were analyzed. The olivine abundance is about 40 vol%. Thus, the inclusion is similar to the refractory inclusions from the ungrouped carbonaceous chondrite Adelaide that were described as “amoeboid olivine aggregates without low-Ca pyroxene” (AOAs) (Krot et al. 2004).

Adrar 003

Adrar 003 is an LL(L)3 chondrite (Wlotzka 1991) whose highly unequilibrated character was recognized immediately (Hutchison et al. 1991; Bischoff et al. 1992). Mineral analyses indicate that olivine compositions range from Fa_7 to Fa_{31} and that pyroxene compositions range from En_{76} to En_{95} (Hutchison et al. 1991). Adrar 003 is one of the most primitive ordinary chondrites according to thermoluminescence (TL) sensitivity data (type 3.1) (Benoit et al. 2002) and Cr contents of ferroan olivine (type 3.10) (Grossman and Brearley 2005).

Several apparently metamorphic fragments were observed among other constituents of Adrar 003 (Figs. 2a and 2b). Some of these objects have textures indistinguishable from those of type 6 chondrites. Most of the fragments, which are very large (~3 mm) (Fig. 2a), contain complete relict barred-olivine chondrules (see especially Fig. 2a) similar in size to chondrules in LL chondrites (~800 μm). The shape and the broken appearance of these fragments indicate that they may represent clasts of larger units. Although similar-looking objects were described as type 2 chondrules (e.g., Kita et al. 2000, personal communication 2007; Mostefaoui et al. 2002), these irregularly shaped inclusions lacking a texture indicating crystallization from a melt cannot be considered to be true chondrules. They are mainly composed of olivine intergrown with pyroxene. Some olivines are in contact with interstitial granular pyroxene. Crystalline feldspar is present as an interstitial phase and is mostly anorthite-rich (Table 1). Olivine and pyroxene show a narrow compositional range ($Fa_{16–19}$ and $Fs_{14–19}$, respectively), indicating significant homogeneity. This homogeneity of the unusual fragments indicates that in contrast to the host rock, they experienced some degree of thermal metamorphism.

Adzhi-Bogdo

Adzhi-Bogdo is an ordinary chondrite regolith breccia (LL3–6) (Bischoff et al. 1993, 1996). It consists of sub-mm to

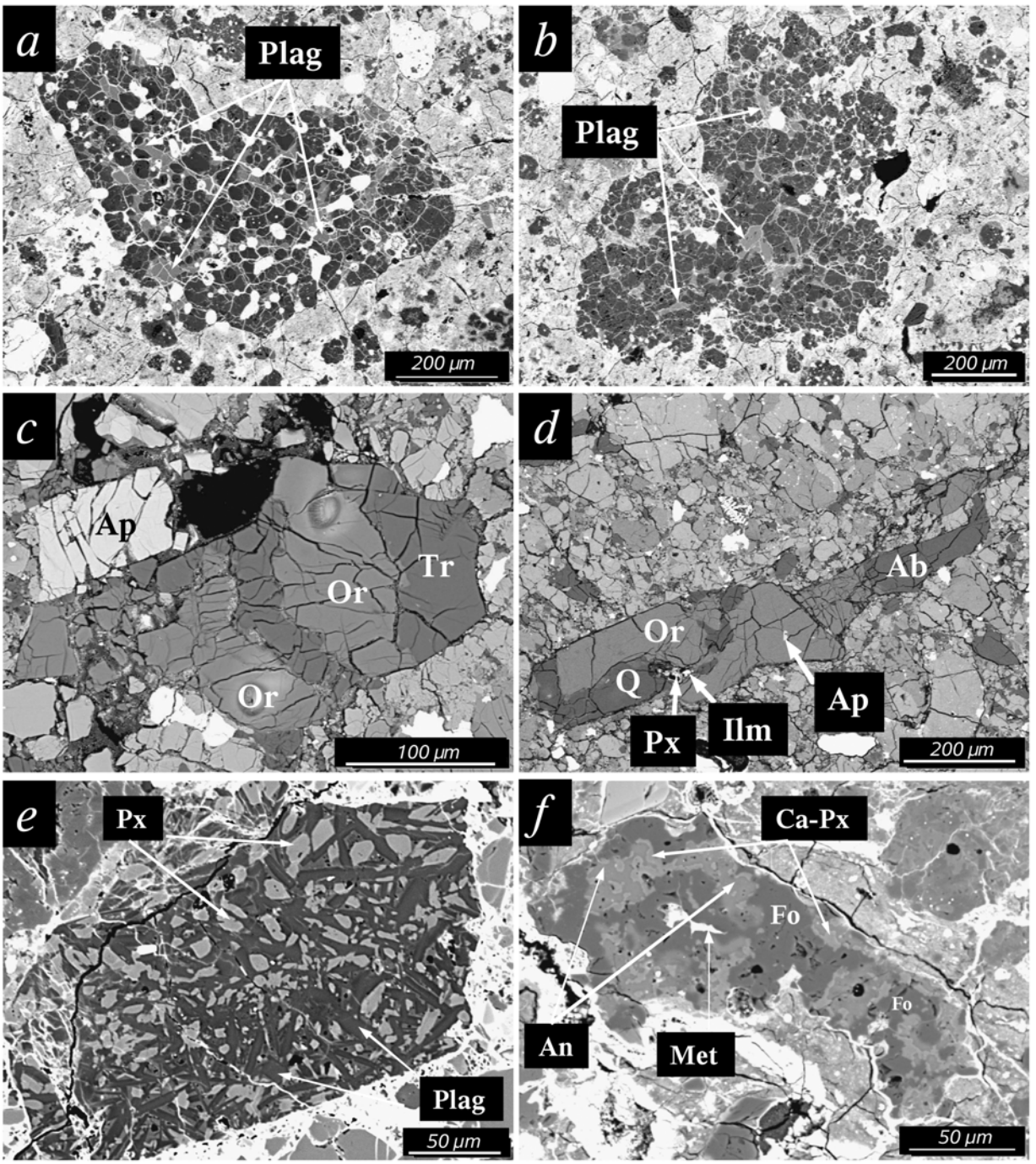

Fig. 1. a) and b) BSE images of analyzed metamorphic fragments from Acfer 094. c) and d) Two granitoidal clasts from Adzhi-Bogdo (#4 and #5). e) The andesitic fragment (1b) and (f) the analyzed Ca-Al-rich inclusion from Acfer 094. Plag = plagioclase, Ab = albite, Px = pyroxene, Ilm = ilmenite, Ap = apatite, Or = orthoclase, Q = quartz, Tr = tridymite, Ca-Px = Ca-pyroxene, Met = Fe,Ni metal, An = anorthite, Fo = forsterite. The objects in (a) and (b) can be described as fragments of units that were once much larger.

cm-sized clasts and chondrules embedded in a fine-grained clastic matrix. This polymict breccia contains different types of fragments, some of which are of foreign origin (Bischoff 1993; Bischoff et al. 1993, 1996, 2006). Constituents include chondrules, melt rock clasts, breccia clasts, highly recrystallized rock fragments ("granulites"), pyroxene-rich fragments with achondritic textures, and alkali-granitoids (Bischoff 1993; Bischoff et al. 1993, 1996). The composition of olivine in most constituents is in the LL range, but olivine in some components is significantly lower in the fayalite component, indicating an L-chondritic origin (Bischoff et al. 1993).

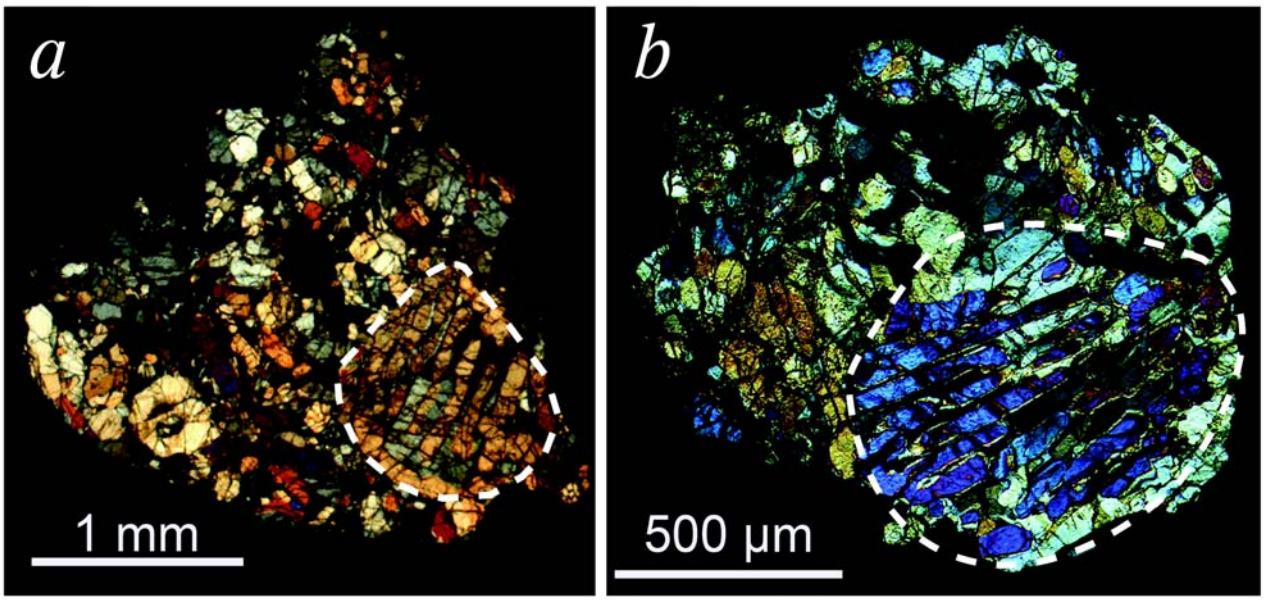

Fig. 2. Metamorphosed fragments with relict barred-olivine chondrules within the unequilibrated ordinary chondrite Adrar 003 (LL3). The fragments are most likely clasts of much larger pre-existing units. Photomicrographs in transmitted light, crossed nicols.

The alkali-granitoid clasts (Figs. 1c and 1d) primarily consist of K-feldspar and SiO_2 phases (tridymite, quartz). Minor phases include albite, Cl-apatite, whitlockite, ilmenite, zircon, Ca-poor pyroxene ($Fs_{66–83}$), and aenigmatite. Fragments #4 and #5 in Figs. 1c and 1d mainly consist of SiO_2 phases, albite, and K-feldspar.

The K-feldspar is almost pure orthoclase ($Or_{96–97}$), and the Na-feldspar has an Ab content of 93.7 mol% (Table 1). In contrast to quartz, which is pure SiO_2, tridymite in these clasts contains on the order of 1.5 wt% Al_2O_3 and 0.8 wt% Na_2O. SiO_2 phases and K-feldspar are coarse-grained and can reach sizes of 700 µm.

The bulk compositions can be calculated based on the mineral compositions and modal abundances (Bischoff 1993). As it is characteristic for granitoids, the fragments are high in SiO_2 (72–79 wt%), Al_2O_3 (11–14 wt%), and K_2O (9–12 wt%), and low in FeO, MgO, and CaO (all below 1 wt%). The K/Na ratio of the granitoid fragments ranges from 5.5 to 32.

Study Butte

Study Butte was originally classified as an H3 chondrite. However, the rock is a breccia (recommended classification: H3–6), consisting of chondrules, matrix, and mineral and lithic fragments (Wlotzka and Fredriksson 1988). Fredriksson et al. (1989) described Study Butte as "an accretionary, well-indurated, multicomponent breccia of exceptional complexity containing a great variety of chondrules and fragments not previously observed in a single stone." Several Ca-Al-rich inclusions and a great variety of different fragments were observed, including one fragment with an andesitic bulk composition (Fredriksson et al. 1989). This fragment (1b) (Fig. 1e) has an igneous texture, which is distinctly different from the textures of chondrules or chondritic lithic fragments from Study Butte. It consists of diopsidic pyroxene and twinned plagioclase. The plagioclase forms a network of primary euhedral crystal laths, in which the pyroxene is interstitial (in chondrules plagioclase is xenomorph and interstitial to pyroxene and/or olivine). The plagioclase ($An_{40–50}$) (Table 1) is more calcic than normal secondary chondritic feldspar (oligoclase) formed during metamorphism and has traces of Fe and Mg, but only about 0.2% K_2O. Interstitial glassy mesostasis is also present (Fredriksson et al. 1989).

In addition to the andesitic fragments, two chondrules having large feldspar crystals were studied (Fig. 3). Chondrule 4a, approximately 80 µm in apparent diameter, is an Al-rich chondrule containing abundant spinel (Fig. 3a). The spinel is rich in Cr_2O_3 and FeO (56 wt% and 31 wt%, respectively). Other major elements detected were 8 wt% Al_2O_3, 4 wt% MgO, and 1 wt% MnO. The spinels are enclosed within feldspars. In some areas the feldspar is oligoclase ($\sim An_{15}Ab_{79}Or_6$), whereas in other portions of the chondrule the feldspar is rich in potassium ($\sim An_5Ab_{58}Or_{27}$) (Table 1). Aluminium chondrules similar in texture or with similar mineral compositions have been found in other ordinary chondrites (Bischoff and Keil 1983, 1984; Bischoff et al. 1989). Chromium-rich spinels were mostly found within metamorphosed ordinary chondrites.

Chondrule 4e is a porphyritic olivine chondrule (Fig. 3b). Euhedral to subhedral olivines and minor low-Ca pyroxene grains are embedded within a fine-grained, crystalline mesostasis consisting of plagioclase and Ca-pyroxene laths. The olivine ($\sim Fa_{18}$) and low-Ca pyroxene ($\sim Fs_{17}$) have compositions typical for olivine and pyroxene in equilibrated

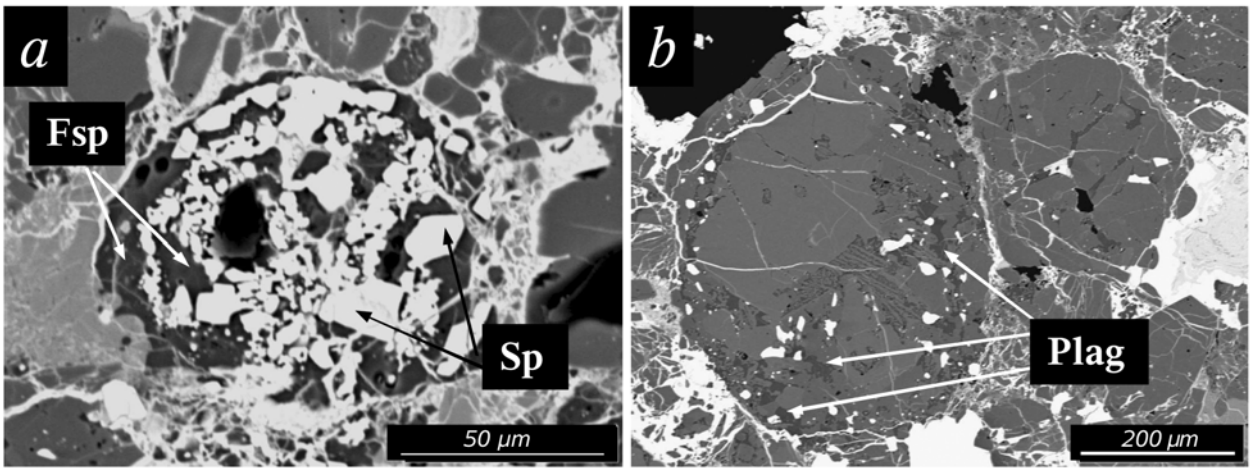

Fig. 3. BSE images of two analyzed chondrules from Study Butte. a) Chondrule 4a is an Al-rich chondrule containing abundant spinel enclosed within feldspars. b) Chondrule 4e is a porphyritic olivine chondrule. Euhedral to subhedral olivines and minor low-Ca pyroxene grains are embedded within a fine-grained, crystalline mesostasis consisting of plagioclase and Ca-pyroxene laths. Fsp = feldspar; Sp = spinel; Plag = plagioclase.

H chondrites. Their homogeneous compositions and the presence of crystallized secondary plagioclase ($An_{10–13}$) indicate that the chondrule has been metamorphosed. Abundant tiny metals and sulfides are scattered throughout the fine-grained portion of the chondrule.

Magnesium Isotopes

Al-Mg results for the 15 inclusions studied are given in Table 2 and plotted in Figs. 4 and 5. Two fragments from Adzhi-Bogdo were measured with the IMS 3f ion probe, whereas four fragments from Adrar 003, three objects from Study Butte, and five fragments and one CAI from Acfer 094 were measured with the NanoSIMS ion microprobe.

In Table 2, the fractionation-corrected excess ^{26}Mg in permil is given relative to the normal ratio $(^{26}Mg/^{24}Mg)_n = 0.13932$ (Catanzaro et al. 1966). Different numbers for a given phase denote different crystals.

$^{26}Mg/^{24}Mg$ ratios measured in olivines and pyroxenes with the NanoSIMS are significantly below the normal value of 0.13932. These low values are not intrinsic to the analyzed phases, but are most likely related to the QSA effect (Slodzian et al. 2004). However, systematic measurements are required to calibrate this effect for Mg measurements. Therefore, all initial $^{26}Al/^{27}Al$ values and upper limits listed in Table 2 (except those for Adzhi-Bogdo) were calculated by forcing the correlation line to pass through the normal $^{26}Mg/^{24}Mg$ ratio at Al/Mg = 0. As pointed out above, the QSA effect is only noticeable in samples with high Mg concentrations and a correction is not necessary for phases with high Al/Mg ratio (see the Analytical Procedures section).

This study reveals isotopically normal Mg in all objects examined (except the CAI from Acfer 094); no clear evidence of radiogenic ^{26}Mg ($^{26}Mg^*$) above the limits of the experimental uncertainty was found in any fragment. If we exclude the CAI from Acfer 094, seven (i.e., 50%) of the 14 analyzed samples have negative slopes. This would be expected from statistical fluctuations if none of these samples have detectable ^{26}Al. In fact, a weighted average of all the ^{26}Mg values, except those for the CAI, gives –0.2 ± 0.9‰. The reduced χ^2 of this fit is 0.98. Similarly, a weighted average of all the slopes obtained for individual samples (except the CAI) in Table 2 gives $(1.2 \pm 13) \times 10^{-7}$ with a reduced χ^2 of 0.98 for this fit. These results show that all data are entirely consistent with isotopically normal Mg, and the variations of the isotopic ratios and the inferred slopes for individual samples can be explained by random statistical fluctuations. Another test was to fit all the data points of these 14 samples to a single line (with errors in both directions). As for the individual samples, we forced the line through normal Mg isotopic composition for Al/Mg = 0. A line with a slope of 1.5×10^{-7} and an error of 1.8×10^{-7} was obtained for this fit. Similarly, the reduced χ^2 of this fit is 0.95. It seems to be very clear that all variations of the data can be explained as statistical fluctuations around normal Mg isotopic compositions and that there is no evidence for any systematic bias in the measurements. Except for the CAI, any evidence for the initial presence of ^{26}Al was found and only upper limits within, unfortunately, relative large uncertainties can be set. These uncertainties are the result of the fine-grained nature and extremely heterogeneous compositions of the samples. We therefore base the estimated upper limits for the $^{26}Al/^{27}Al$ ratio on the error for the individual samples. However, in order to be on the safe side, we added a possible systematic uncertainty based on the following reasoning: although the data are entirely consistent with normal Mg, the measurement on the standards gave an average of –1.5‰ for $\delta^{26}Mg$. If this represents a systematic shift for all $\delta^{26}Mg$

Table 2. Results of Mg isotope analyses.

Meteorite	Mineral	$^{27}Al/^{24}Mg$	$\delta^{26}Mg$	$(^{26}Al/^{27}Al)_0$	Upper limit[a]	Time diff.[b] (Myr)
Adzhi Bogdo #4	Or 1	1910 ± 160	−3 ± 10			
	Or 2	2330 ± 190	0 ± 18			
	Or 3	1350 ± 110	2 ± 10			
	Or 4	1560 ± 120	3.2 ± 9.6			
	Px 1	0.027 ± 0.004	−0.5 ± 2.4	$(0.7 \pm 4.9) \times 10^{-7}$	$(5.6 + 1.2) \times 10^{-7}$	4.5
Adzhi Bogdo #5	Or 1	1950 ± 140	2 ± 11			
	Or 2	1990 ± 150	−1 ± 14			
	Or 3	1910 ± 170	−10 ± 14			
	Or 4	1860 ± 180	6 ± 13			
	Px 1	0.03 ± 0.003	−1.1 ± 2.6			
	Px 2	0	0.4 ± 7.6			
	Px 3	0	−0.9 ± 5.4	$(-0.4 \pm 4.9) \times 10^{-7}$	$(4.9 + 1.1) \times 10^{-7}$	4.7
Acfer 094 #1	Plag 1	36.8 ± 3.9	−1.9 ± 6.4			
	Plag 2	59.9 ± 3.9	1.5 ± 5.5			
	Plag 3	35.9 ± 2.3	0.6 ± 6.3			
	Plag 4	60.2 ± 4.0	2.2 ± 5.6			
	Plag 5	32.6 ± 2.1	3.5 ± 9.1	$(3.3 \pm 8.3) \times 10^{-6}$	$(1.2 + 0.5) \times 10^{-5}$	1.1
Acfer 094 #2	Plag 1	45.1 ± 3.9	1.1 ± 6.4			
	Plag 2	44.8 ± 3.1	2.0 ± 7.9			
	Plag 3	36.9 ± 3.1	−1.4 ± 5.9			
	Plag 4	39.1 ± 3.2	−7.0 ± 7.5	$(-3.4 \pm 12) \times 10^{-6}$	$(1.5 + 0.5) \times 10^{-5}$	1.0
Acfer 094 #3	Plag 1	27.9 ± 1.7	−5.5 ± 5.3			
	Plag 2	33.5 ± 2.1	3.5 ± 5.0			
	Plag 3	32.1 ± 2.0	−1 ± 15			
	Plag 4	28.1 ± 1.8	0.2 ± 4.7	$(-0.7 \pm 19) \times 10^{-6}$	$(1.9 + 0.7) \times 10^{-5}$	0.7
Acfer 094 #10	Plag 1	275 ± 29	27 ± 71			
CAI	Plag 2	722 ± 46	42 ± 29			
	Plag 3	325 ± 23	45 ± 26			
	Plag 4	612 ± 54	25 ± 96	$(1.0 \pm 0.5) \times 10^{-5}$	$(1.5 + 0.0) \times 10^{-5}$	1.3
Acfer 094 #4	Plag 1	47.8 ± 3.8	0.1 ± 4.9			
	Plag 2	74.2 ± 6.5	−3.2 ± 4.5			
	Plag 3	37.8 ± 4.0	0.9 ± 4.1			
	Plag 4	44.2 ± 3.6	−2.9 ± 5.6	$(-3.8 \pm 6.6) \times 10^{-6}$	$(6.6 + 4.1) \times 10^{-6}$	1.6
Acfer 094 #5	Plag 1	28.6 ± 2.8	−2.7 ± 3.4			
	Plag 2	24.1 ± 0.5	−3.8 ± 3.7			
	Plag 3	37.6 ± 3.1	−0.5 ± 3.5	$(-8.8 \pm 10.2) \times 10^{-6}$	$(1.0 + 0.7) \times 10^{-5}$	1.1
Adrar 003 #1	Plag 1	43.7 ± 7.9	−5 ± 11			
	Plag 2	35.9 ± 6.4	2.5 ± 7.8			
	Plag 2	33.7 ± 5.8	0.9 ± 4.6			
	Plag 2	52.7 ± 9.4	2.1 ± 6.0			
	Plag 5	38.3 ± 6.8	2.5 ± 3.3	$(5.9 \pm 8.7) \times 10^{-6}$	$(1.5 + 0.5) \times 10^{-5}$	1.0
Adrar 003 #2	Plag 1	82.4 ± 10.6	−1 ± 10			
	Plag 2	51.7 ± 8.0	2 ± 10			
	Plag 3	56.7 ± 3.6	1.5 ± 5.7			
	Plag 4	55.3 ± 3.7	1.7 ± 4.1			
	Plag 5	55.4 ± 3.6	0.2 ± 5.3			
	Plag 6	97.4 ± 6.8	1.2 ± 7.1	$(2.4 \pm 5.8) \times 10^{-6}$	$(8.2 + 3.1) \times 10^{-6}$	1.6
Adrar 003 #3	Plag 1	31.7 ± 6.3	8.4 ± 5.9			
	Plag 2	57.8 ± 10.0	10 ± 38			
	Plag 3	49.0 ± 8.5	0.1 ± 5.4	$(1.0 \pm 1.4) \times 10^{-5}$	$(2.4 + 0.5) \times 10^{-5}$	0.6
Adrar 003 #4	Plag 1	47.1 ± 20.6	1 ± 15			
	Plag 2	50.6 ± 8.8	0 ± 10			
	Plag 3	40.2 ± 7.1	−2.9 ± 6.9			
	Plag 4	48.9 ± 8.5	−3.9 ± 6.8	$(-0.7 \pm 1.3) \times 10^{-5}$	$(1.3 + 0.4) \times 10^{-5}$	1.1

Table 2. *Continued.* Results of Mg isotope analyses.

Meteorite	Mineral	$^{27}Al/^{24}Mg$	$\delta^{26}Mg$	$(^{26}Al/^{27}Al)_0$	Upper limit[a]	Time diff.[b] (Myr)
Study Butte #1b	Plag 1	2360 ± 170	17.1 ± 29.5			
	Plag 2	2230 ± 850	−7.0 ± 30			
	Plag 3	6600 ± 2100	4 ± 75			
	Plag 4	2800 ± 1100	10 ± 38	$(2.7 \pm 8.8) \times 10^{-7}$	$(1.2 + 0.1) \times 10^{-6}$	3.8
Study Butte #4a	Plag 1	1390 ± 100	7 ± 32			
	Plag 1	690 ± 61	−5 ± 13			
	Plag 3	1036 ± 97	16.7 ± 74.7			
	Plag 4	4450 ± 360	−7 ± 35			
	Plag 5	2390 ± 410	−4 ± 49	$(-2.2 \pm 9.1) \times 10^{-7}$	$(9.1 + 1.0) \times 10^{-7}$	4.1
Study Butte #4e	Plag 1	8900 ± 1170	0 ± 66			
	Plag 2	8900 ± 1200	6 ± 43			
	Plag 3	6820 ± 540	33.1 ± 26.2			
	Plag 4	6310 ± 440	−9 ± 18			
	Plag 5	6580 ± 430	27.2 ± 19.0	$(2.6 \pm 3.5) \times 10^{-7}$	$(6.1 + 0.3) \times 10^{-7}$	4.6

[a]The upper limits have two contributions. The first expresses the uncertainty derived from the data; the second expresses a shift due to a possible systematic bias in the $\delta^{26}Mg$ measurements. See text.

[b]The lower time difference between the canonical value and the value estimated for the sample is based on the total upper limit on the $^{26}Al/^{27}Al$ ratio.

Errors equated with data are 2σ. The initial $(^{26}Al/^{27}Al)_0$ was calculated from the slope of the correlation line. Fragments from Adzhi Bogdo were measured with the IMS 3f ion probe, fragments from Acfer 094, Adrar 003, and Study Butte with the NanoSIMS ion microprobe. Pyroxene data reported for Adzhi Bogdo were obtained from the matrix of the meteorite. Isochrons based on NanoSIMS data were forced to pass through the normal $^{26}Mg/^{24}Mg$ ratio at Al/Mg = 0. Different numbers for a given phase denote different crystals; Or = orthoclase, Px = pyroxene, Plag = plagioclase.

values, the slopes of the correlation lines would be systematically higher, depending on the $^{27}Al/^{24}Mg$ ratios. In column 6 of Table 2 we therefore give two components for the upper limit, the first representing the uncertainty derived from the data, and the second expressing the effect of a possible systematic shift in the $\delta^{26}Mg$ values. The age difference given in column 7 is based on the total upper limit.

The analyzed orthoclase grains in both fragments from Adzhi-Bogdo have $^{27}Al/^{24}Mg$ ratios from 1350 to 2330. In spite of these very high Al/Mg ratios, no ^{26}Mg excess was detected. Because of their small size, it was not possible to measure pyroxenes as the phase with a low Al/Mg ratio in the fragments. Instead, pyroxenes in the matrix were analyzed and they showed normal Mg isotope compositions. The initial $^{26}Al/^{27}Al$ ratios determined from the slope of the correlation lines are $(0.7 \pm 4.9) \times 10^{-7}$ for fragment 4 and $(-0.4 \pm 4.9) \times 10^{-7}$ for fragment 5. Calculated upper limits are $(5.6 + 1.2) \times 10^{-7}$ and $(4.9 + 1.1) \times 10^{-7}$, respectively (Table 2).

The measured $^{27}Al/^{24}Mg$ values of the plagioclase phases in the metamorphic fragments from Acfer 094 are in the range of 24–74, which unfortunately is quite low and results in fairly large uncertainties for the inferred $^{26}Al/^{27}Al$ ratios. The Mg isotopic compositions of these fragments are normal within the limits of the experimental uncertainties. No evidence for radiogenic ^{26}Mg can be observed. The upper limits are listed in Table 2. The analysis of the small anorthite grains in the CAI from Acfer 094 was hampered by contribution to the Mg signal from the surrounding Mg-rich, low-Al phases. In spite of the relatively large experimental uncertainty, a ^{26}Mg excess could be detected. The data yield an inferred value of $(1.0 \pm 0.5) \times 10^{-5}$.

None of the four fragments with metamorphic texture from Adrar 003 show clear evidence for ^{26}Mg excess, but the limits on $(^{26}Al/^{27}Al)_0$ permitted by the data are not particularly tight. The Al/Mg ratios in measured plagioclases are low (ranging from 32 to 97) and result in large uncertainties for the inferred $^{26}Al/^{27}Al$ ratios. The upper limits on the $^{26}Al/^{27}Al$ ratios range from $(8.2 + 3.1) \times 10^{-6}$ to $(2.4 + 0.5) \times 10^{-5}$.

The andesitic fragment from Study Butte has quite high Al/Mg ratios, ranging from 2230 to 6600. Four distinct feldspar grains were measured, but no ^{26}Mg excesses (above the limits of the experimental uncertainty) could be detected. The model isochron exhibits a positive slope of $(2.7 \pm 8.8) \times 10^{-7}$. The upper limit on $(^{26}Al/^{27}Al)_0$ is $(1.2 + 0.1) \times 10^{-6}$.

The two analyzed chondrules from Study Butte (4a and 4e) show no clear evidence for ^{26}Mg excess. In chondrule 4e, two plagioclase grains show resolved excess in ^{26}Mg. However, if all measured grains are considered, the inferred $(^{26}Al/^{27}Al)_0$ is $(2.6 \pm 3.5) \times 10^{-7}$. Chondrule 4a gives an initial $(^{26}Al/^{27}Al)$ ratio of $(-2.2 \pm 9.1) \times 10^{-7}$ with an upper limit of $(9.1 + 1.0) \times 10^{-7}$.

DISCUSSION

Constraints on the Accretion Time of Chondrite Parent Bodies

Both Acfer 094 and Adrar 003 are characterized as highly unequilibrated chondrites. They contain chondrules and clasts set in a fine-grained, opaque matrix. The textural appearance as well as the chemical homogeneity of the fragments supports the conclusion that several components

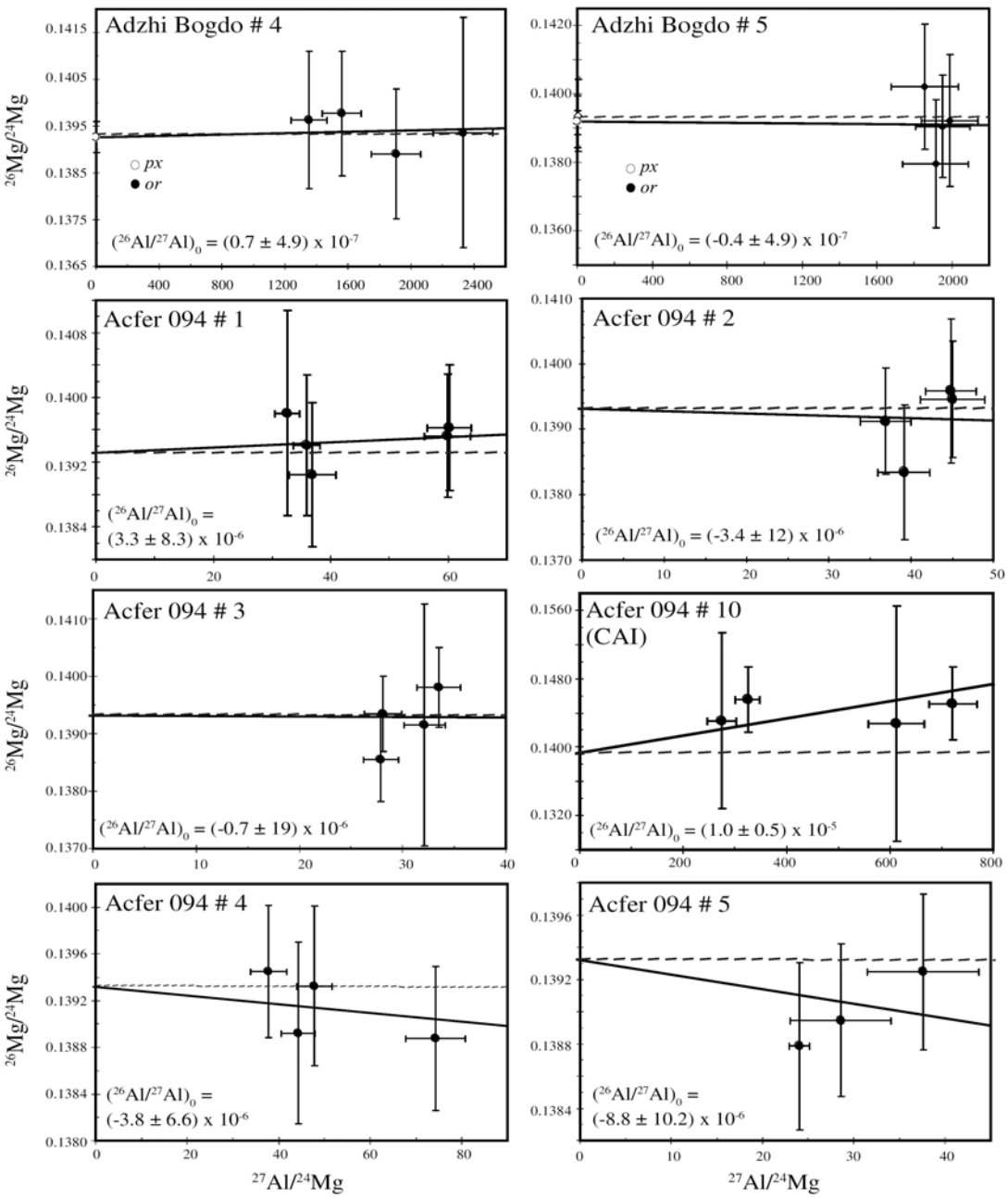

Fig. 4. $^{27}Al/^{24}Mg$ versus $^{26}Mg/^{24}Mg$ plots for eight analyzed fragments. Errors plotted are 2σ. The dashed horizontal line represents the normal $^{26}Mg/^{24}Mg$ ratio. The slope of the correlation line corresponds to the initial $^{26}Al/^{27}Al$ ratio for these objects. Correlation lines were forced to pass through the normal $^{26}Mg/^{24}Mg$ ratio at Al/Mg = 0 (except data from Adzhi-Bogdo).

were affected by thermal annealing that led to equilibration of the phases within the fragments but not in host rocks. Since both meteorites are type 3 chondrites, the metamorphosed fragments must have been heated prior to incorporation into the present matrix. This metamorphic imprint may have occurred on a precursor parent body. In fragments from Adrar 003, the thermal overprint was probably not strong enough to destroy all chondritic features; relict barred-olivine chondrules can still be observed in these fragments (Fig. 2).

None of the analyzed metamorphic fragments show clear evidence for ^{26}Mg excesses. It is possible that they never had any ^{26}Al or that their ^{26}Al clock was reset during thermal metamorphism. However, they consist of phases with low Al/Mg ratios (Table 2) (see the Analytical Procedures section), making it difficult to detect small amounts of radiogenic ^{26}Mg using ion probe techniques. The calculated upper limits on $^{26}Al/^{27}Al$ range from $(8.2 + 3.1) \times 10^{-6}$ to $(2.4 + 0.5) \times 10^{-5}$ (corresponding to a time of 0.6–

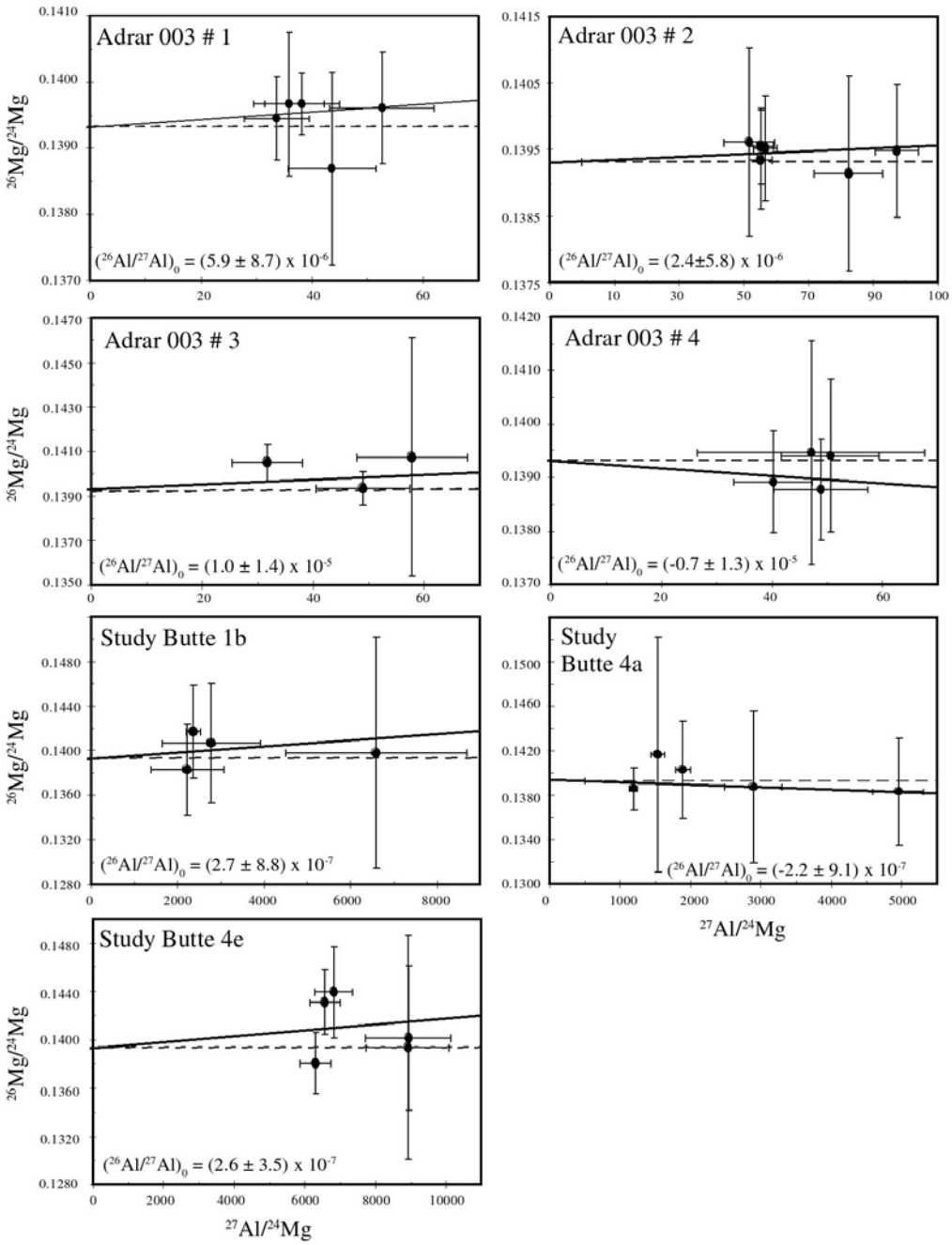

Fig. 5. $^{27}Al/^{24}Mg$ versus $^{26}Mg/^{24}Mg$ plots for seven analyzed fragments. Errors plotted are 2σ. The dashed horizontal line represents normal $^{26}Mg/^{24}Mg$ ratio. The slope of the correlation line corresponds to the initial $^{26}Al/^{27}Al$ ratio for these objects. Correlation lines were forced to pass through the normal $^{26}Mg/^{24}Mg$ ratio at Al/Mg = 0.

1.6 Myr after CAI formation) in fragments from Adrar 003. Metamorphism of the inclusions in Acfer 094 certainly postdates the formation of CAIs by at least 0.7–1.6 Myr (as calculated from upper limits on the $^{26}Al/^{27}Al$ ratio) (Table 2). This profound thermal overprint must have occurred before the incorporation of these fragments into their present parent bodies, since the parent bodies themselves escaped thermal metamorphism.

In two anorthite-rich chondrules from Acfer 094, Hutcheon et al. (2000) reported ^{26}Mg excesses corresponding to an initial $^{26}Al/^{27}Al$ ratio of $(1.2 \pm 0.4) \times 10^{-5}$ (~1.5 Myr after CAIs). Sugiura and Krot (2006) reported nearly canonical initial $^{26}Al/^{27}Al$ ratios in 11 CAIs and in anorthite from an igneous "amoeboid olivine aggregate"–like object extracted from Acfer 094. Three other CAIs, two of them of a refractory nature and one with

an igneous texture, have no resolvable excesses in ^{26}Mg. The igneous-textured CAI may have experienced late-stage remelting before incorporation into the final parent body (Sugiura and Krot 2006). The metamorphosed lithic fragment containing a Ca-Al-rich inclusion described by Bischoff et al. (2006) and analyzed by Krot et al. (2006) also shows no ^{26}Mg excess. The CAI measured in the present study exhibits an initial ^{26}Al/^{27}Al ratio of $(1.0 \pm 0.5) \times 10^{-5}$ (Table 2), which corresponds to an age of ~1.7 Ma relative to the canonical value, and within the uncertainties is almost identical to the $(^{26}Al/^{27}Al)_0$ ratio of the two chondrules measured by Hutcheon et al. (2000).

The fact that the CAI measured in this study shows a similar age as the two chondrules measured by Hutcheon et al. (2000) may indicate that the CAI was remelted during the chondrule-forming event. The existence of the igneous-textured CAI with no resolvable ^{26}Mg excess (Sugiura and Krot 2006) may indicate a further heating event.

Obviously, Acfer 094 contains components with different histories and ages, possibly even several populations of CAIs. Accretion of the Acfer 094 parent body must have occurred after the formation of its youngest components and thus must have been relatively late. Thus, despite the primitive nature of Acfer 094, the presence of Al-rich material with no resolvable ^{26}Mg excesses in this meteorite implies that its parent body accreted after most of the ^{26}Al had decayed.

The possibility of the metamorphic fragments being remnants of an impactor (which collided with the Acfer 094 parent body some time after the accretion of Acfer 094) seems to be highly unlikely, because the meteorite itself as well as the inclusions are apparently unshocked (S1) (Newton et al. 1995). Furthermore, primitive accretionary breccias such as Acfer 094 are thought to consist of constituents that were assembled during the formation of breccia parent bodies (Bischoff et al. 2006). Thus, it is more likely these fragments were present at the time of accretion of Acfer 094 and it is likely that they are derived from early formed, thermally modified, and disrupted planetesimals.

Rudraswami and Goswami (2007) reported Al-Mg data for chondrules from Adrar 003. One chondrule yielded an initial ^{26}Al/^{27}Al of $(0.63 \pm 0.4) \times 10^{-5}$, while another one showed a value of $(0.84 \pm 0.78) \times 10^{-5}$. These ratios correspond to an age of ~2.2 Ma after CAI formation. These results and the existence of fragments with no resolvable ^{26}Mg excess in this study demonstrate that Adrar 003 also accreted rather late (at least 2.2 Ma after CAIs formed) in spite of its primitive nature. Furthermore, the occurrence of metamorphosed chondritic fragments (as indicated by relict chondrules in the described fragments) in the LL-chondrite parent body indicates that chondrite accretion was a multistage process and thus possibly took place over an extended period of time. Such chondritic clasts may be derived from early formed planetesimals and may indicate the existence of chondritic precursor planetesimals.

If accretion and differentiation of planetesimals started prior to or contemporaneously with chondrule formation, as stated by Kleine et al. (2005a, 2005b) and Bizzarro et al. (2005), it cannot be ruled out that some of the planetary material (e.g., metamorphosed fragments, chondritic clasts) could have been ejected and incorporated into later-formed chondritic parent bodies, especially because collisions between objects were common in the early solar system (e.g., Bunch and Rajan 1988; Chambers 2006). Some breccias (primitive, accretionary breccias) are thought to result from mixing of material from disrupted (precursor) parent bodies. A completely foreign, slightly metamorphosed chondritic clast in Krymka is a convincing example (see Fig. 3 in Bischoff et al. [2006]). A black microchondrule- and carbon-bearing L-like chondritic fragment was found in the Mezö-Madaras L3 chondritic breccia (Christophe Michel-Lévy 1988). A similar clast with tiny chondrules was found in Krymka (LL3) (Rubin 1989). However, the late accretion of the analyzed chondrites may even account for their primitive nature in the sense that the abundance of ^{26}Al at the time of accretion was too low to thermally modify the parent body.

If chondrite parent body formation was a multistage process, one can assume that chondrule formation was a multistage process as well. This in turn implies that the formation process took place over an extended time scale that overlapped with other early planetary processes such as igneous differentiation and core formation. Since chondrules with ages of ~4 Ma after CAI formation exist (Russell et al. 1997; CB chondrules, Krot et al. 2005; Sanders and Taylor 2005), the chondrule-forming events may have occurred as multiple short episodes at least during the first 4 Myr of the early solar system. However, if the parent body formation of Acfer 094 and Adrar 003 was late, the primitive matrix as well as CAIs having the canonical ^{26}Al/^{27}Al ratios must have been stored over an extended period of time. Hutchison et al. (2005) suggested storage (of CAIs and presolar grains) in small bodies or near-surface layers in larger bodies. In the case of small bodies, they must have been small enough to escape heating by ^{26}Al, but large enough (~10 km) (Shu et al. 1997) to resist inward drift to the protosun.

Occurrence and Origin of Igneous-Textured Fragments

Adzhi-Bogdo contains several igneous-textured inclusions that are best described as alkali-granitoids. Coarse-grained, granite-like inclusions also occur in Vishnupur (LL4–6) (Wlotzka et al. 1983). Most likely, these fragments formed from a melt and crystallized slowly enough to allow the formation of large quartz/tridymite and orthoclase crystals. According to Fredriksson et al. (1989) the igneous-textured fragment in Study Butte (fragment 1b) (Fig. 1e) has an andesitic bulk composition. Andesites are igneous, volcanic rocks with an intermediate (between felsic and mafic) composition. Almost identical inclusions occur in the

Beddgelert H5 chondrite (Fredriksson et al. 1989). Both the granitoids and the andesite are igneous clasts that appear to have been formed by magmatic differentiation on a parent body in response to extensive heating and melting. While the coarse crystals in the granitoids indicate slow cooling, the finer grain size of the andesite points toward a lava-type rock.

The Mg isotopes for two fragments from Adzhi-Bogdo (AB #4 and AB #5) do not show evidence for radiogenic ^{26}Mg. The calculated upper limits for the ^{26}Al/^{27}Al ratio are $(5.6 + 1.2) \times 10^{-7}$ (AB #4) and $(4.9 + 1.1) \times 10^{-7}$ (AB #5). These limits refer to the ^{26}Al/^{27}Al ratios that correspond to the time when the rocks had cooled enough for Mg diffusion to have ceased, which is at least 4.7 Myr after CAIs had formed.

Plagioclase in fragment 1b from Study Butte has also no detectable radiogenic ^{26}Mg. The upper limit for ^{26}Al/^{27}Al is $(1.2 + 0.1) \times 10^{-6}$, indicating that this clast did not cool until at least ~4 Myr after CAIs had formed. Two chondrules from Study Butte appear to have been thermally modified. The upper limits of $(9.1 + 1.0) \times 10^{-7}$ and $(6.1 + 0.3) \times 10^{-7}$ for ^{26}Al/^{27}Al correspond to ages of 4.1 Myr and 4.6 Myr after CAI formation.

The possibility that evidence for ^{26}Al was erased by parent-body metamorphism after incorporation of the fragments in their present parent bodies is not likely because these fragments and several other constituents (e.g., chondrules and mineral components) of Adzhi-Bogdo and Study Butte do not indicate whole rock equilibration or recrystallization. The presence of interstitial glassy mesostasis in the andesitic fragment (Fredriksson et al. 1989) supports this assumption, since glass would not have survived metamorphism. Therefore, incorporation of the fragments into their present matrix occurred late, after almost all ^{26}Al had decayed.

Oxygen isotopes of phases in the andesite from Study Butte and three fragments from Adzhi-Bogdo were analyzed by Sokol et al. (2007). The data of all fragments fall in the range of ordinary chondrites but show significant variations. The igneous fragments certainly do not derive from known differentiated parent bodies represented by other achondrites.

Due to the distinct oxygen isotope variations it is not clear whether the melt from which the fragments crystallized formed on the LL or H chondrite parent body itself, or whether these fragments formed on another planetary body. If these fragments formed on the parent body itself, there are two options for heat and melt generation: internal heating (e.g., due to ^{26}Al decay) or impact heating. Since ^{26}Al was active only in the first few million years, its abundance may have been too low to cause large-scale melting and differentiation on the chondritic parent bodies (assuming a late accretion of chondritic parent bodies); otherwise, the Al-rich phases that crystallized from these melts should show evidence for the decay of ^{26}Al. Furthermore, it is generally accepted that chondritic parent bodies from which type 3 to type 6 chondrites derive did not melt and that the temperatures they achieved was just enough for metamorphism. Thus, extensive melting and differentiation due to ^{26}Al decay in the parent bodies of the chondritic breccias Adzhi-Bogdo and Study Butte is unlikely.

Folco et al. (2004) noted that hypervelocity cosmic impacts during the early bombardment that affected the inner solar system could have provided the necessary energy for large-scale melting on chondritic bodies. These impacts could have generated a number of different lithologies on the H chondrite parent body, ranging from basaltic and gabbroic achondrites to irons, depending on the degree of metal-silicate segregation and depth of crystallization. According to Folco et al. (2004), a plausible setting for such a magmatic differentiation process might be impact melt sheets at a crater floor that can have generated an upper silicate and a lower metal layer.

It has also been suggested that impacts on asteroids that are less than a few hundred kilometers in diameter cannot have been the heat source for melt generation and do not mix much projectile material into the target (e.g., Love and Ahrens 1996; Keil et al. 1997). In particular, there is no evidence to support the idea that the H and LL chondrite parent bodies were more than a few hundred kilometers in diameter. Additionally, Keil et al. (1997) suggested that single asteroidal impacts will generate only very small melt volumes and that internal differentiation is not observed in any impact melt rocks.

Alternatively, the igneous fragments may have formed by magmatic activity on other planetary bodies. In this case, they may represent parts of parent bodies not yet sampled. Again, melt generation may be due to impact heating or decay of ^{26}Al. Bizzarro et al. (2005) noted that the achondrite parent bodies accreted and differentiated while ^{26}Al was sufficiently abundant to cause asteroid melting. In contrast, accretion of chondrite parent bodies began relatively late, i.e., after most ^{26}Al had decayed (>2 Myr after CAI formation) and heat production had become insufficient to melt asteroids. Thus, if these older pre-existing bodies accreted early (during the lifetime of ^{26}Al), they may have been melted and differentiated as predicted by the model of Bizzarro et al. (2005). Thermal modeling by Hevey and Sanders (2006) and Sanders and Taylor (2005) indicate that decay of ^{26}Al would have melted bodies that formed within 1.5 Myr after CAI formation and whose radius exceeds 20 to 80 km (depending on the time of accretion). Such bodies would have cooled and solidified within 4 Myr. Larger bodies were able to retain the heat for longer periods of time. Thus, if the early formed bodies were large enough, widespread melting could have persisted for an extended period of time. Cooling and crystallization of the studied igneous fragments may have been late (~3.8 Myr and 4.7 Myr after CAIs formed) so that the evidence for ^{26}Al as a heat source in the igneous objects was erased. High-velocity impacts may have disrupted these early differentiated bodies and transported the igneous fragments to their present parent bodies.

It is not clear if the igneous fragments represent individual objects during accretion or if they were incorporated into their present parent bodies at a later stage. If they represent individual objects during accretion, the Al-Mg data indicate that accretion of the parent bodies of Adzhi-Bogdo as well as of Study Butte was late, i.e., after almost all ^{26}Al had decayed (as indicated by the calculated upper limits). If these fragments represent remnants of an achondritic projectile, the time of accretion of the chondritic breccias cannot be constrained. Nevertheless, the lack of significant radiogenic ^{26}Mg in the fragments requires an assembly in their present form after almost all ^{26}Al had decayed.

In either case, it seems clear that impacts and collisions between planetary bodies are an important mechanism of planetary accretion. They may or may not produce large amounts of melt, but are a crucial process for the evolution of planetesimals and are responsible for breccia formation (Bischoff et al. 2006). Independently of the place and way of formation, impacts must have been responsible for the incorporation of the igneous fragments into the present host rocks.

Impacts were also considered to play an important role during chondrule formation by disruption of at least partially molten planetesimals (e.g., Hevey and Sanders 2006; Sanders and Taylor 2005; Hutchison et al. 2005). According to these authors, disruption of such bodies would have produced huge clouds of melt droplets, i.e., chondrules. Chondrite parent bodies may have formed out of the debris of the disrupted "first generation" parent bodies and chondrules.

Neither the granitoids nor the andesitic fragments contain any features of impact metamorphism. Thus, if the origin of the igneous fragment was a foreign body, the speed at which they encountered the present parent body must have been low. Additionally, the presence of similar fragments in other chondrites (granite-like inclusions in Vishunpur LL4–6 and andesitic inclusions in Beddgelert H5) may indicate that the sources of the granitoids as well as the andesites were close to their present parent bodies.

CONCLUSIONS

The metamorphic and igneous objects found in a matrix of significantly lower grade do not show evidence for the presence of ^{26}Al during crystallization. Only upper limits for the ^{26}Al/^{27}Al ratio could be established. In Acfer 094, the upper limits on the ^{26}Al/^{27}Al indicate a thermal overprint of some fragments at least 1.6 Myr after the CAI formed. The upper limits in fragments from Adrar 003 correspond to 0.6–1.6 Myr after the CAI formed. Some other components in these meteorites also show no resolvable ^{26}Mg excess (e.g., CAIs in Acfer 094) (Krot et al. 2006; Sugiura and Krot 2006). Since final accretion of a planetesimal must have occurred after formation of its youngest components, formation of Acfer 094 and Adrar 003 parent bodies must thus have been relatively late (i.e., after most ^{26}Al had decayed). Furthermore, the occurrence of metamorphosed chondritic fragments (relict chondrules in the fragments) in the LL-chondrite parent body (Adrar 003) indicates that chondrite parent body accretion was a multistage process and thus took place over an extended period of time.

The absence of ^{26}Mg excess in the igneous inclusions from Adzhi-Bogdo and Study Butte does not exclude ^{26}Al from being a heat source for planetary melting. In large, early formed planetesimals, cooling below the closure temperature of the Al-Mg system may be too late for any evidence for live ^{26}Al (in the form of ^{26}Mg excess) to be preserved. Thus, these fragments may have formed on early formed and differentiated bodies and may have been ejected and incorporated into their present matrix at a later stage.

So far, all evidence for the existence of "old" differentiated objects derives from measurements on bulk samples and calculated model ages. No differentiated objects showing Al-Mg isochron ages that are older than chondrule ages have been reported.

Impacts and collisions between planetary bodies are an important mechanism during planetary accretion and evolution. Growing evidence exists that chondrites considered as unequilibrated, primitive, and pristine (e.g., Semarkona, Krymka, Acfer 094, etc.) have a very complicated history and were formed by mixing of various chondritic (e.g., foreign chondritic fragment in Krymka) (Bischoff et al. 2006) and minor nonchondritic components (e.g., CC-1 from Semarkona) (Hutcheon and Hutchison 1989) with different formation ages. Some aggregates found in chondrites consist of material from diverse sources with different metamorphic, magmatic, and differentiation histories, which were finally combined to form the meteorite parent bodies.

Acknowledgments–We thank Tim Smolar for technical assistance; Tim McCoy (Smithsonian Institution; National Museum of Natural History, Washington) for the loan of the Study Butte thin section; and Christine Floss for discussions, help, and support during the NanoSIMS experimental work, and for organizing Anna K. Sokol's visit to St. Louis. This study is part of the dissertation of Anna K. Sokol and was also supported by NASA grant NNG04GG49G and by a grant of the German Research Foundation (DFG; ME 1717/4-3). We also wish to thank Noriko Kita and an anonymous reviewer for their constructive comments and helpful suggestions that resulted in a significantly improved manuscript.

Editorial Handling—Dr. Ian Lyon

REFERENCES

Amelin Y., Krot A. N., Hutcheon I. D., and Ulyanov A. A. 2002. Lead isotopic ages of chondrules and calcium-aluminum-rich inclusions. *Science* 297:1678–7683.

Baker J. and Bizzarro M. 2005. ^{26}Mg-deficit dating of differentiated meteorites with Al/Mg ~ 0: Accretion and melting of protoplanets in the first million years of the solar system (abstract #1286). Proceedings, Protostars and Planets V.

Baker J., Bizzarro M., Witting N., Connelly J., and Haack H. 2005. Early planetesimal melting from an age of 4.5662 Gyr for differentiated meteorites. *Nature* 436:1127–1131.

Benoit P. H., Akridge G. A., Ninagawa K., and Sears D. W. G. 2002. Thermoluminescence sensitivity and thermal history of type 3 ordinary chondrites: Eleven new type 3.0–3.1 chondrites and possible explanations for differences among H, L, and LL chondrites. *Meteoritics & Planetary Science* 37:793–805.

Bischoff A. 1993. Alkali-granitoids as fragments within the ordinary chondrite Adzhi-Bogdo: Evidence for highly fractionated, alkali-granitic liquids on asteroids (abstract). 24th Lunar and Planetary Science Conference. pp. 113–114.

Bischoff A. 1998. Aqueous alteration of carbonaceous chondrites: Evidence for pre-accretionary alteration. A review. *Meteoritics & Planetary Science* 33:1113–1122.

Bischoff A. and Geiger T. 1994. The unique carbonaceous chondrite Acfer 094: The first CM3 chondrite (?) (abstract). 25th Lunar and Planetary Science Conference. pp. 115–116.

Bischoff A. and Keil K. 1983. *Catalog of Al-rich chondrules, inclusions and fragments in ordinary chondrites*. UNM Institute of Meteoritics Special Publication #22. Albuquerque, New Mexico: University of New Mexico. 29 p.

Bischoff A. and Keil K. 1984. Al-rich objects in ordinary chondrites: Related origin of carbonaceous and ordinary chondrites and their constituents. *Geochimica et Cosmochimica Acta* 48:693–709.

Bischoff A., Palme H., and Spettel B. 1989. Al-rich chondrules from the Ybbsitz H4 chondrite: Evidence for formation by collision and splashing. *Earth and Planetary Science Letters* 93:170–180.

Bischoff A., Palme H., Clayton R. N., Mayeda T. K., Grund T., Spettel B., Geiger T., Endress M., Beckerling W., and Metzler K. 1991. New carbonaceous and type 3 ordinary chondrites from the Sahara desert. *Meteoritics* 26:318–319.

Bischoff A., Sears D. W. G., Benoit P. H., Geiger T., and Stöffler D. 1992. New type 3 chondrites from the Sahara Desert (abstract). 23rd Lunar and Planetary Science Conference. pp. 107–108.

Bischoff A., Geiger T., Palme H., Spettel B., Schultz L., Scherer P., Schlüter J., and Lkhamsuren J. 1993. Mineralogy, chemistry, and noble gas contents of Adzhi-Bogdo—An LL3–6 chondritic breccia with foreign clasts. *Meteoritics* 28:570–578.

Bischoff A., Gerel O., Buchwald V. F., Spettel B., Loeken T., Schultz L., Weber H. W., Schlüter J., Baljinnyam L., Borchuluun D., Byambaa C., and Garamjav D. 1996. Meteorites from Mongolia. *Meteoritics & Planetary Science* 31:152–157.

Bischoff A., Weber D., Spettel B., Clayton R. N., Mayeda T. K., Wolf D., and Palme H. 1997. Hammadah al Hamra 180: A unique unequilibrated chondrite with affinities to LL-group ordinary chondrites (abstract). *Meteoritics & Planetary Science* 32:A14.

Bischoff A. and Schultz L. 2004. Abundance and meaning of regolith breccias among meteorites (abstract). *Meteoritics & Planetary Science* 39:A15.

Bischoff A., Scott E. R. D., Metzler K., and Goodrich C. A. 2006. Nature and origins of meteoritic breccias. In *Meteorites and the early solar system II*, edited by Lauretta D. S. and McSween H. Y., Jr. Tucson, Arizona: The University of Arizona. pp. 679–712.

Bizzarro M., Baker J. A., and Haack H. 2005. Rapid time scales for accretion and melting of differentiated planetesimals inferred from ^{26}Al-^{26}Mg chronometry. *The Astrophysical Journal* 632: L41–L44.

Bridges J. C. and Hutchison R. 1997. A survey of clasts and chondrules in ordinary chondrites. *Meteoritics & Planetary Science* 32:389–394.

Bridges J. C., Franchi I. A., Hutchison R., Morse A. D., Long J. V. P., and Pillinger C. T. 1995a. Cristobalite- and tridymite-bearing clasts in Parnallee (LL3) and Farmington (L5). *Meteoritics* 30: 715–727.

Bridges J. C., Hutchison R., Franchi I. A., Alexander C. M. O'D., and Pillinger C. T. 1995b. A feldspar-nepheline achondrite clast in Parnallee. *Proceedings of the NIPR Symposium on Antarctic Meteorites* 8:195–203.

Bunch T. E. and Rajan R. S. 1988. Meteorite regolith breccias. In *Meteorites and the early solar system*, edited by Kerridge J. F. and Matthews M. S. Tucson, Arizona: The University of Arizona. pp. 144–164.

Catanzaro E. J., Murphy T. J., Garner E. L., and Shields W. R. 1966. Absolute isotopic abundance ratios and atomic weight of magnesium. *Journal of Research of the National Institute of Standards and Technology* 70A:453–458.

Chambers J. 2006. Meteoritic diversity and planetesimal formation. In *Meteorites and the early solar system II*, edited by Lauretta D. S. and McSween H. Y., Jr. Tucson, Arizona: The University of Arizona. pp. 487–497.

Christophe Michel-Lévy M. 1988. A new component of the Mezö-Madaras breccia: A microchondrule- and carbon-bearing L-related chondrite. *Meteoritics* 23:45–48.

Folco L., Bland P. A., D'Orazio M., Franchi I. A., Kelley S., and Rocchi S. 2004. Extensive impact melting on the H-chondrite parent asteroid during the cataclysmic bombardment of the early solar system: Evidence from the achondritic meteorite Dar al Gani 896. *Geochimica et Cosmochimica Acta* 68:2379–2397.

Fredriksson K., Jarosewich E., and Wlotzka F. 1989. Study Butte: A chaotic chondrite breccia with normal H-group chemistry. *Zeitschrift für Naturforschung* 44a:945–962.

Gao X., Amari S., Messenger S., Nittler L. R., Swan P. D., and Walker R. M. 1996. Survey of circumstellar grains in the unique carbonaceous chondrite Acfer 094 (abstract). *Meteoritics & Planetary Science* 31:A48.

Greshake A. 1997. The primitive matrix components of the unique carbonaceous chondrite Acfer 094: A TEM study. *Geochimica et Cosmochimica Acta* 61:437–452.

Grossman J. N. and Brearley A. J. 2005. The onset of metamorphism in ordinary and carbonaceous chondrites. *Meteoritics & Planetary Science* 40:87–122.

Haack H., Baker J. A., and Bizzarro M. 2005 Accretion of differentiated asteroids—Before, during, or after chondrule formation (abstract)? *Meteoritics & Planetary Science* 40:A62.

Hevey P. J. and Sanders I. S. 2006. A model for planetesimal meltdown by ^{26}Al and its implications for meteorite parent bodies. *Meteoritics & Planetary Science* 41:95–106.

Hezel D. 2003. Die Bildung SiO_2-reicher Phasen im frühen Sonnensystem. Ph.D. thesis, Universität zu Köln, Germany.

Huss G. R., MacPherson G. J., Wasserburg G. J., Russell S. S., and Srinivasan G. 2001. Aluminium-26 in calcium-aluminium-rich inclusions and chondrules from unequilibrated ordinary chondrites. *Meteoritics & Planetary Science* 36:975–997.

Hutcheon I. D. and Hutchison R. 1989. Evidence from the Semarkona ordinary chondrite for ^{26}Al heating of small planets. *Nature* 337:238–241.

Hutcheon I. D., Krot A. N., and Ulyanov A. A. 2000. ^{26}Al in anorthite-rich chondrules in primitive carbonaceous chondrites: Evidence chondrules post-date CAI (abstract #1869). 31st Lunar and Planetary Science Conference. CD-ROM.

Hutchison R. 1996. Chondrules and their associates in ordinary chondrites: A planetary connection. In *Chondrules and the protoplanetary disk*, edited by Hewins R. H., Jones R. H., and Scott E. R. D. Cambridge, England: Cambridge University Press. pp. 311–318.

Hutchison R., Williams C. T., Din V. K., Clayton R. N., Kirschbaum C., Paul R. L., and Lipschutz M. E. 1988. A planetary, H-group pebble in the Barwell, L6, unshocked chondritic meteorite. *Earth and Planetary Science Letters* 90: 105–118.

Hutchison R., Reed S. J. B., Ash R. D., and Pillinger C. T. 1991. Adrar 003: A new extraordinary unequilibrated ordinary chondrite (abstract). *Meteoritics* 26:349.

Hutchison R., Bridges J. C., and Gilmour J. D. 2005. Chondrules: Chemical, petrographic, and chronologic clues to their origin by impact. In *Chondrites and the protoplanetary disk*, edited by Krot A. N., Scott E. R. D., and Reipurth B. ASP Conference Series #341. San Francisco: Astronomical Society of the Pacific. pp. 933–950.

Keil K., Stöffler D., Love S. G., and Scott E. R. D. 1997. Constraints on the role of impact heating and melting in asteroids. *Meteoritics & Planetary Science* 32:349–363.

Kennedy A. K., Hutchison R., Hutcheon I. D., and Agrell S. O. 1992. A unique high Mn/Fe microgabbro in the Parnallee (LL3) ordinary chondrite: Nebular mixture or planetary differentiate form a previously unrecognized planetary body? *Earth and Planetary Science Letters* 113:191–205.

Kita N. T., Nagahara H., Togashi S., and Morishita Y. 2000. A short duration of chondrule formation in the solar nebula: Evidence from ^{26}Al in Semarkona ferromagnesian chondrules. *Geochimica et Cosmochimica Acta* 64:3913–3922.

Kita N. T., Huss G. R., Tachibana S., Amelin Y., Nyquist L. E., and Hutcheon I. D. 2005. Constraints on the origin of chondrules and CAIs from short-lived and long-lived radionuclides. In *Chondrites and the protoplanetary disk*, edited by Krot A. N., Scott E. R. D., Reipurth B. ASP Conference Series #341. San Francisco: Astronomical Society of the Pacific. pp. 558–587.

Kleine T., Mezger K., Palme H., Scherer E., and Münker C. 2004. A new chronology for asteroid formation in the early solar system based on ^{182}W systematics (abstract #P31C-04). *Eos* 85.

Kleine T., Mezger K., Palme H., and Scherer E. 2005a. Tungsten isotopes provide evidence that core formation in some asteroids predates the accretion of chondrite parent bodies (abstract #1431). 36th Lunar and Planetary Science Conference. CD-ROM.

Kleine T., Mezger K., Palme H., Scherer E., and Münker C. 2005b. A new model for the accretion and early evolution of asteroids in the early solar system: Evidence from ^{182}Hf-^{182}W in CAIs, metal-rich chondrites, and iron meteorites. *Geochimica et Cosmochimica Acta* 69:5805–5818.

Krot A. N., Petaev M. I., and Yurimoto H. 2004. Amoeboid olivine aggregates with low-Ca pyroxenes: A genetic link between refractory inclusions and chondrules? *Geochimica et Cosmochimica Acta* 68:1923–1941.

Krot A. N., Amelin Y., Cassen P., and Meibom A. 2005. Young chondrules in CB chondrites from a giant impact in the early solar system. *Nature* 436:989–992.

Krot A. N., McKeegan K. D., Huss G. R., Liffman K., Sahijpal S., Hutcheon I. D., Srinivasan G., Bischoff A., and Keil K. 2006. Aluminum-magnesium and oxygen isotope study of relict Ca-Al-rich inclusions in chondrules. *The Astrophysical Journal* 639: 1227–1237.

Kunihiro T., Rubin A. E., McKeegan K. D., and Wasson J. T. 2004. Initial ^{26}Al/^{27}Al in carbonaceous-chondrite chondrules: Too little ^{26}Al to melt asteroids. *Geochimica et Cosmochimica Acta* 68: 2947–2957.

Libourel G. and Krot A. N. 2007. Evidence for the presence of planetesimal material among the precursors of magnesian chondrules of nebular origin. *Earth and Planetary Science Letters* 254:1–8.

Love S. G. and Ahrens T. J. 1996. Catastrophic impacts on gravity dominated asteroids. *Icarus* 124:141–155.

Markowski A., Quitte G., Halliday A. N., and Kleine T. 2006. Tungsten isotopic compositions of iron meteorites: Chronological constraints versus cosmogenic effects. *Earth and Planetary Science Letters* 242:1–15.

Misawa K., Watanabe S., Kitamura M., Nakamura N., Yamamoto K., and Masuda A. 1992. A noritic clast from the Hedjaz chondritic breccia: Implications for melting events in the early solar system. *Geochemical Journa*l 26:435–446.

Mittlefehldt D. W., Lindstrom M. M., Wang M.-S., and Lipschutz M. E. 1995. Geochemistry and origin of achondritic inclusions in Yamato-75097, -793241, and -794046 chondrites. *Proceedings of the NIPR Symposium on Antarctic Meteorites* 8: 251–271.

Mostefaoui S., Kita N. T., Togashi S., Tachibana S., Nagahara H., and Morishita Y. 2002. The relative formation ages of ferromagnesian chondrules inferred from their initial aluminum-26/aluminum-27 ratios. *Meteoritics & Planetary Science* 37: 421–438.

Nagao K. 1994. Noble gases in hosts and inclusions from Yamato-75097 (L6), -793241 (L6), and -794046 (H5). *Proceedings of the NIPR Symposium on Antarctic Meteorites* 7:197–216.

Nakamura N., Misawa K., Kitamura M., Masuda A., Watanabe S., and Yamamoto K. 1990. Highly fractionated REE in the Hedjaz (L) chondrite: Implications for nebular and planetary processes. *Earth and Planetary Science Letters* 99:290–302.

Newton J., Bischoff A., Arden J. W., Franchi I. A., Geiger T., Greshake A., and Pillinger C. T. 1995. Acfer 094, a uniquely primitive carbonaceous chondrite from the Sahara. *Meteoritics* 30:47–56.

Nguyen A. N. and Zinner E. 2004. Discovery of ancient silicate stardust in a meteorite. *Science* 303:1496–1499.

Nguyen A. N., Stadermann F. J., Zinner E., Stroud R. M., Alexander C. M. O'D., and Nittler L. R. 2007. Characterization of presolar silicate and oxide grains in primitive carbonaceous chondrites. *The Astrophysical Journal* 656:1223–1240.

Prinz M., Nehru C. E., Weisberg M. K., Delany J. S., Yanai K., and Kojima H. 1984. H-chondritic clasts in a Yamato L6 chondrite: Implications for metamorphism. *Meteoritics* 19:292–293.

Rubin A. E. 1989. An olivine-microchondrule–bearing clast in the Krymka meteorite. *Meteoritics* 24:191–192.

Rudraswami N. G. and Goswami J. N. 2007. ^{26}Al in chondrules from unequilibrated L chondrites: Onset and duration of chondrule formation in the early solar system. *Earth and Planetary Science Letters* 257:231–244.

Russell S. S., Srinivasan G., Huss G. R., Wasserburg G. J., and MacPherson G. J. 1996. Evidence for widespread ^{26}Al in the solar nebula and constraints for nebula time scales. *Science* 273:757–762.

Russel S. S., Huss G. R., MacPherson G. J., and Wasserburg G. J. 1997. Early and late chondrule formation: New constraints for solar nebula chronology from ^{26}Al/^{27}Al in unequilibrated ordinary chondrites (abstract #1468). 28th Lunar and Planetary Science Conference. CD-ROM.

Ruzicka A., Kring D. A., Hill D. H., Boynton W. V., Clayton R. N., and Mayeda T. K. 1995. Silica-rich orthopyroxenite in the Bovedy chondrite. *Meteoritics* 30:57–70.

Ruzicka A., Snyder G. A., and Taylor L. A. 1998. Mega-chondrules and large, igneous-textured clasts in Julesberg (L3) and other ordinary chondrites: Vapor-fractionation, shock-melting, and chondrule formation. *Geochimica et Cosmochimica Acta* 62: 1419–1442.

Sanders I. S. 1996. A chondrule-forming scenario involving molten planetesimals. In *Chondrules and the protoplanetary disk*, edited

by Hewins R. H., Jones R. H., Scott E. R. D. Cambridge: Cambridge University Press. pp. 327–334.

Sanders I. S. and Taylor G. J. 2005. Implications of ^{26}Al in nebular dust: Formation of chondrules by disruption of molten planetesimals. In *Chondrites and the protoplanetary disk*, edited by Krot A. N., Scott E. R. D., and Reipurth B. ASP Conference Series #341. San Francisco: Astronomical Society of the Pacific. pp. 915–932.

Shu F. H., Shang H., Glassgold A. E., and Lee T. 1997. X-rays and fluctuating X-winds from protostars. *Science* 277:1475–1479.

Slodzian G., Hillion F., Stadermann F. J., and Zinner E. 2004. QSA influences on isotopic ratio measurements. *Applied Surface Science* 231–232:874–877.

Sokol A. K. and Bischoff A. 2006. Simultaneous accretion of differentiated or metamorphosed asteroidal clasts and chondrules (abstract). *Meteoritics & Planetary Science* 41:A164.

Sokol A. K., Mezger K., Chaussidon M., and Bischoff A. 2007. Achondritic fragments in ordinary chondrite breccias (abstract). *Meteoritics & Planetary Science* 42:A143.

Srinivasan G., Goswami J. N., and Bhandari N. 1999. ^{26}Al in eucrite Piplia Kalan: Plausible heat source and formation chronology. *Science* 284:1348–1350.

Sugiura N. and Krot A. N. 2006. Al-Mg dating of Ca-Al-rich inclusions in Acfer 094 chondrite (abstract #1265). 37th Lunar and Planetary Science Conference. CD-ROM.

Urey H. C. 1959. Primary and secondary objects. *Journal of Geophysical Research* 64:1721–1737.

Urey H. C. 1967. Parent bodies of the meteorites and origin of chondrules. *Icarus* 7:350–359.

Wlotzka F. 1991. The Meteoritical Bulletin. *Meteoritics* 26:255–262.

Wlotzka F. and Fredriksson K. 1988. Magnetite-carbide and Al-rich inclusions in the Study Butte H3-chondrite. *Meteoritics* 23:311–312.

Wlotzka F., Palme H., Spettel B., Wänke H., Fredriksson K., and Noonan A. F. 1983. Alkali differentiation in LL chondrites. *Geochimica et Cosmochimica Acta* 47:743–757.

Zanda B. 2004. Chondrules. *Earth and Planetary Science Letters* 224:1–17.

Zinner E., Hoppe P., and Lugmair G. 2002. Radiogenic ^{26}Mg in the Ste Marguerite and Forest Vale plagioclase: Can ^{26}Al be used as chronometer? (abstract #1204) 33rd Lunar and Planetary Science Conference. CD-ROM.

Zook H. A. 1980. A new impact model for the generation of ordinary chondrites. *Meteoritics* 15:390–391.